Physiologia Plantarum
An International Journal for Plant Biology

Physiologia Plantarum 151: 112–118. 2014

A high-throughput imaging auxanometer for roots and hypocotyls of *Arabidopsis* using a 2D skeletonizing algorithm

Simon Fraas, Vera Niehoff and Hartwig Lüthen*

Biozentrum Flottbek der Universität, Ohnhorststr. 18, Hamburg, 22609, Germany

Correspondence
*Corresponding author,
e-mail: h.luthen@botanik.uni-hamburg.de

Received 13 January 2014;
revised 5 March 2014

doi:10.1111/ppl.12183

Next generation phenotyping of auxin response mutants will be greatly facilitated by the ability to record rapid growth responses in roots and hypocotyls at high throughput and at high temporal resolution. As *Arabidopsis* seedlings are very tiny and fragile, imaging is the only adequate way for data acquisition. As camera-based systems described before have a limited throughput, we used commercial flatbed scanners to record a large number of simultaneous experiments. We developed Hansa Trace, software for automatically detecting and measuring hypocotyl segments and roots in the images. We validated this system by measuring some well-characterized growth responses to auxins, non-auxins, ATPase activators and apoplastic acidification. The method can be shared on a cooperation basis and is able to perform measurements with minimal user intervention.

Introduction

Auxin growth responses are very dramatic and very rapid effects. They occur after a short lag phase of <10 to 20 min. Correlating them with molecular data (e.g. quantitative polymerase chain reaction or chip-based transcriptional kinetics) requires measuring systems permitting high temporal and spatial resolution. The receptors responsible for the effect are not unequivocally identified. The effect still occurs in mutants in which most of the transport inhibitor response 1 (TIR1) and auxin receptor f-box protein (AFB) receptors have been knocked out (Schenck et al. 2010), while mutant roots are reasonably auxin-insensitive (Scheitz et al. 2013). A role of auxin-binding protein 1 (ABP1) in rapid auxin-induced growth has been suggested but remains unproven. The target genes of the ABP1 and TIR1 pathways leading to rapid auxin-induced growth effects are also not identified by now.

Arabidopsis gave new chances and new challenges to auxinology. Hypocotyl segment tests in excised, auxin-depleted segments were a commonplace in the history of auxin research since the 1920s (e.g. Went 1928). Measuring auxin-induced growth at a high temporal resolution was easy with maize coleoptiles or soybean hypocotyls. Beginning in the 1970s, positional and angular transducers were used to record growth responses (for a review of this older work, see Evans 1974), and these systems, for the first time, gave a very high time resolution in the order of minutes. Later, modern AD converters and data acquisition systems made it possible to operate transducer-based auxanometers in series to acquire a bulk of data in a short time (e.g. Claussen et al. 1997). However, transducers require sturdy hypocotyls and coleoptile segments. Because of the technical difficulties in achieving an adequate time resolution, growth tests in *Arabidopsis* were often performed by ruler and after an incubation time of 24–48 h.

Abbreviations – 2,4-D, 2,4-dichlorophenoxyacetic acid; AFB, auxin receptor f-box protein; CCD, charge-coupled device; CIS, compact image sensor; FC, fusicoccin; HT, Hansa Trace; IAA, indole-3-acetic acid; TIR1, transport inhibitor response 1; ABP1, auxin-binding protein 1.

The tiny hypocotyl segments of *Arabidopsis* clearly call for optical, imaging-based approaches. There have been a number of attempts to use cameras for recording growth responses of *Arabidopsis* roots and hypocotyls since 1990 (Ishikawa et al. 1991, Evans et al. 1994, Christian and Lüthen 2000, Schenck et al. 2010). However, these systems still require a degree of manual interaction for the user, which limits their throughput. In an era of genomics and next-generation sequencing, there is a general need for next-generation phenotyping (review: Cobb et al. 2013). For the analysis of rapid auxin-induced elongation growth, this means that responses in a lot of interesting mutants need to be recorded at various different auxin concentrations and experimental conditions. The bulk of experimental runs cannot be handled by conventional camera-based imaging and image analysis techniques. To overcome this limitation, we developed a scanner-based auxanometer that can record growth responses in a large number of *Arabidopsis* roots or hypocotyl segments simultaneously. For analyzing the data, we developed Hansa Trace (HT), a plugin for the ImageJ/Fiji platform. Together, these changes permit a large increase of throughput at an acceptable accuracy and time resolution.

Materials and methods

Choice of the imaging system: use of a flatbed scanner

Most existing imaging systems for auxanometers use microscopes (Fig. 1A), digital cameras or digitizing video cameras (Fig. 1B). We did not follow these lines. Microscopes (Fig. 1A) offer an excellent resolution, but a small field of view (Fig. 1 D). Macro cameras (Fig. 1B, E), when used at a sufficient resolution, cover a larger, but still insufficient field. A large array of industry cameras could potentially overcome this obstacle. However, we also found that the amount of handling (illumination, focusing, etc.) became a key time-consuming factor.

We therefore shifted from microscopes and macroscopic cameras to conventional flatbed scanners (Fig. 1C). Consumer flatbed scanners cover an enormous field of view (Fig. 1F, typically DIN A4, (210 × 297 mm) at reasonable resolution (up to 4800 × 9600 dpi) or more. One can arrange a large number of measuring cuvettes or Petri dishes on its ground glass, making scanners an ideal choice for high-throughput work. Charge-coupled device (CCD) models, unlike compact image sensor (CIS) models, also offer a depth of field of

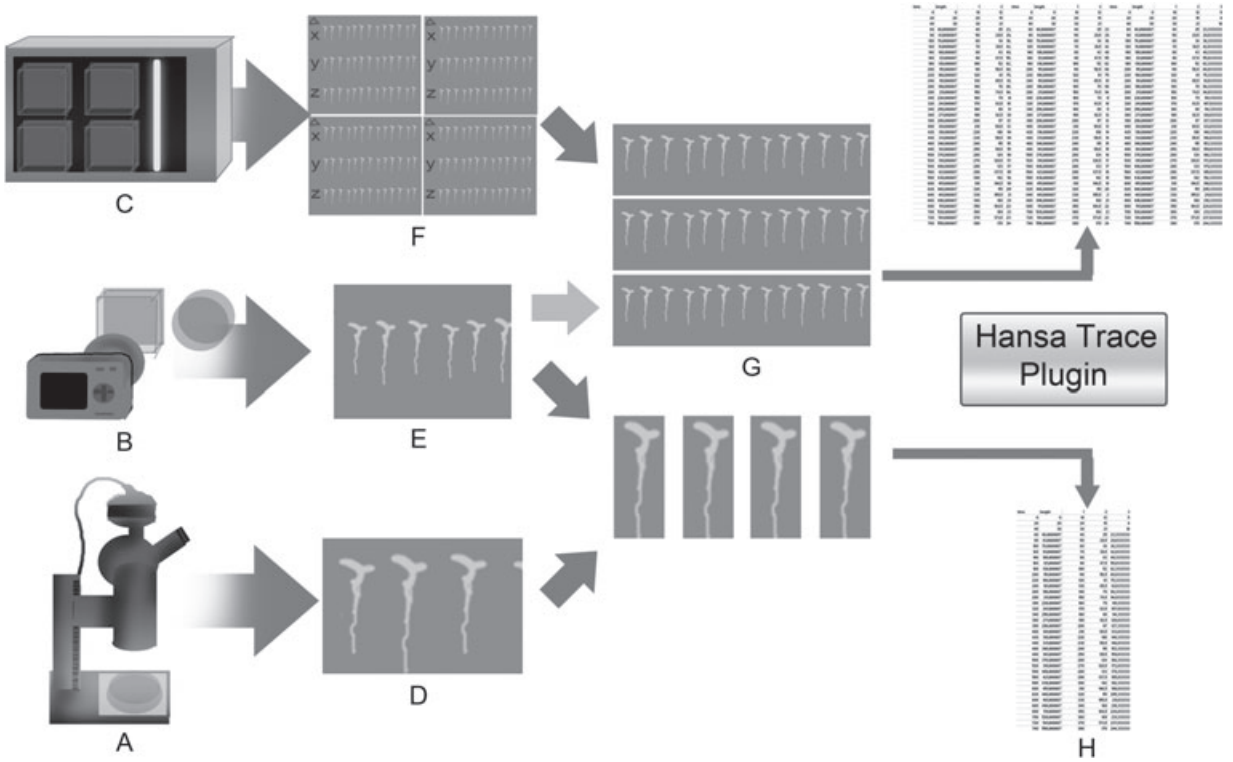

Fig. 1. Scheme of the HT plugin functionality. Imaging can be done by micrographic camera (A), macro cameras (B) and scanners (C). The scanner covers a very large field of view (F) compared with the microscope (D) and the macro camera (E). The images are cropped (G). Thresholding, skeletonization as well as determination of the largest shortest path (the root or segment length) are carried out by the plugin (H).

several millimeters, avoiding the need of precise focusing typical for camera or microscope systems (Fig. 1F). We used an Epson Perfection V30 scanner for our experiments. Macro software was used to acquire scans at regular intervals every 10–20 min (Boxwech 2, Oliver Reuter, Baden-Baden, Germany, http://www.gshow.de/downloads/boxwech2/download.html). Images were stored as TIF files at 8-bit depth in monochrome mode.

Experimental setup for roots

Arabidopsis seeds were placed on 1.5% agar (10 m*M* KCl, 1 m*M* $CaCl_2$) in 10 × 10 cm parafilm-sealed square Petri dishes, stored at 4°C for 2 days for stratification. During germination and growth, the plates were placed vertically in 12-h light conditions.

The plates were placed on the scanner that was positioned vertically (Fig. 2A, B). On the ground glass, the Petri dishes could be inserted at reproducible positions on a self-made adapter plate. Auxins and fusicoccin were added by spraying the plants with the affector solutions [indole-3-acetic acid, IAA, K^+-salt in water (Merck, Darmstadt, Germany), 2,4-dichlorophenoxyacetic acid (2,4-D) and 2,3-D and fusicoccin (FC) (Sigma, Deisenhofen, Germany) were dissolved in small amounts of isopropanol and then diluted to the desired concentration]. All other details were described elsewhere (Scheitz et al. 2013).

Experimental setup for hypocotyls

Col-0 and mutant seeds were sown on moist paper (No. 2048, Schleicher & Schuell, Dassel, Germany) in Parafilm-sealed Petri dishes. Seeds were stratified for 3 days at 4°C in darkness, irradiated with white light for 16 h and kept for 2 days at 26°C in dark. All other details are described elsewhere (Schenck et al. 2010). In order to deplete the segments of endogenous auxin, the tip of the hypocotyls including the cotyledons and the apical hook was removed and segments, 5 mm in length and including the elongation zone, were cut and used for the experiments. The segments were collected in 10 m*M* KCl, 1 m*M* $CaCl_2$ solution. This medium was also used for the experiments. Affectors were applied by adding aliquots of stocking solutions prepared as described above.

For the induction of acid growth, the diffusion barrier of the cuticula had to be removed by abrasion. Hypocotyls were vortexed in a suspension of 600 mesh SiC powder (Karl Schriever, Hamburg, Germany; 0.5 g in 5 ml of water) for 20–30 s. No visible dead cells were detected by staining in Evans Blue, whereas a strong staining with neutral red indicated a high percentage of cells open to the incubation medium (for details, refer to Lüthen et al. 1990).

For imaging, we used a horizontal scanner equipped with a 24-well plate (128 × 86 mm with round wells;

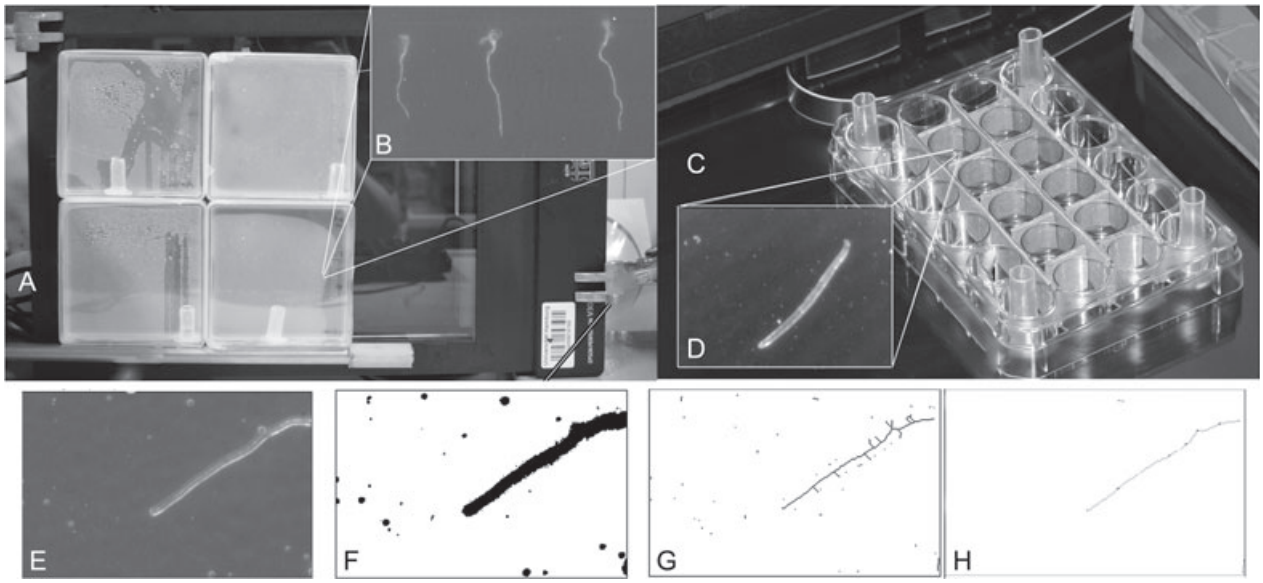

Fig. 2. Experimental setup for measuring growth of intact primary roots of *Arabidopsis*. Agar plates containing the seedlings are positioned on a vertically oriented scanner (A). Elongation responses of hypocotyl segments could be recorded by placing the segments in multi-well plates (C). Typical portion of a scanned image is shown in the insets (B, D). (E–H) The steps of the automatic processing workflow performed on a raw image of a root tip (E): thresholding (F), skeletonizing (G). (H) The longest shortest path identified by the software.

Nunclon delta 14247 (Thermo Fisher Scientific, Langenselbold, Germany). A single segment was placed in each well on the surface of 0.5 ml incubation medium. Adhesion and cohesion form a meniscus on the surface of the solution. We found that relatively short segments are held in place by surface tension in the center of this meniscus (Fig. 2B, C). Care must be taken that the elongation zone is completely included in the segment. More recently, we use floaters, which have a central aperture and which are made of black plastic to prevent longer segments from floating too close to the edges of the well. Gravitropic curvature did not appear to be a factor in the decapitated segments used here.

HT-Plugin for ImageJ and Fiji

For analyzing the elongation growth, we developed a plugin for ImageJ, the Java-based open-source image processing and analysis program, called HT. We used the 64-bit Fiji ImageJ version (http://fiji.sc/Fiji). The script is written in the ImageJ macro language. It is compatible with images from microscopes (Fig. 1A, D, G, H), cameras (Fig. 1B, E, G, H) and scanners (Fig. 1C, F–H), but our main focus was on scanner-based imaging. Briefly, images containing individual or several plants or segments (Fig. 1G) were cropped from the raw data. The plugin then determine the length of the root or segment and stores this data to a *.csv-file to be further processed in MS Excel or Microcal Origin V.9.1. The basic steps of the script are thresholding and skeletonizing of the hypocotyl segments or root images. In the last step, the shortest longest path is identified to determine the length of the object.

Thresholding

A reproducible and uniform thresholding algorithm is essential for automatic and unattended measuring, as the threshold influences the detected length of the segment. We tried various algorithms available within Fiji and ImageJ and found that the Triangle algorithm (Zack et al. 1977) yielded the most robust output. In some cases, the default routine (based on iterative intermean) and especially the maximum entropy algorithm (Kapur et al. 1985) gave good results.

Skeletonizing and longest shortest path determination

HT uses the 2D–3D skeletonizing implemented in Fiji (Lee et al. 1994). Fig. 2E, F shows the effects of thresholding and skeletonizing (Fig. 2G).

HT determines the shortest longest path utilizing Fiji's Analyze Skeleton tool (Arganda-Carreras et al. 2010, Polder et al. 2010). Briefly, this plugin tags all pixel/voxels in a skeleton image and then counts all its junctions, triple and quadruple points and branches, and measures their average and maximum length (Fig. 2H). The longest path was identified using a self-written routine that gives the length of the hypocotyl segments or root.

Statistics

For presenting the data, Microcal Origin 9.1 was used. Briefly, we normalized the segment or root length to the start of the experiments. Arithmetic means and standard errors were then computed. Original data and statistical treatment of control are shown in Fig. S1, Supporting Information.

Results

A number of experiments were performed to validate the system and to characterize the responses of *Arabidopsis* roots and coleoptiles.

Responses of roots to auxin and fusicoccin

Fig. 3A shows the response of *Arabidopsis* (Col-0) root elongation to 10^{-5} *M* IAA. As expected, a rapid inhibition of growth could be observed. This response is auxin-specific, as 2,4-D, but not 2,3-D, induced the inhibition (Fig. 3B). Note that the curves shown are based on 20 individual roots measured simultaneously. Fusicoccin, an activator of the H^+-ATPase proton pump, had no effect (Fig. 3C). This is surprising at the first glance, but can be expected, as maize roots have been shown to respond very weakly to apoplastic acidification and to Fusicoccin (Lüthen and Böttger 1988, 1993). Lüthen and Böttger (1988) report a stimulation of maize root elongation by 40%, while in decapitated maize coleoptiles an increase by some 500% was detected (Lüthen et al. 1990).

Hypocotyls respond to auxins, fusicoccin and apoplastic acidification

In hypocotyls, the active auxin IAA rapidly induced elongation growth in a dose-dependent manner (Fig. 4A). A growth stimulation could also be triggered by 10^{-5} *M* 2,4-D (Fig. 4B). In hypocotyls, an apoplastic acidification to pH 4 by applying citrate buffer induced a transient growth response (Fig. 4C). To our knowledge, rapid time courses of acid growth have never been shown before in the tiny segments of *Arabidopsis*. The initial rise in growth rate was followed by shrinkage, the latter

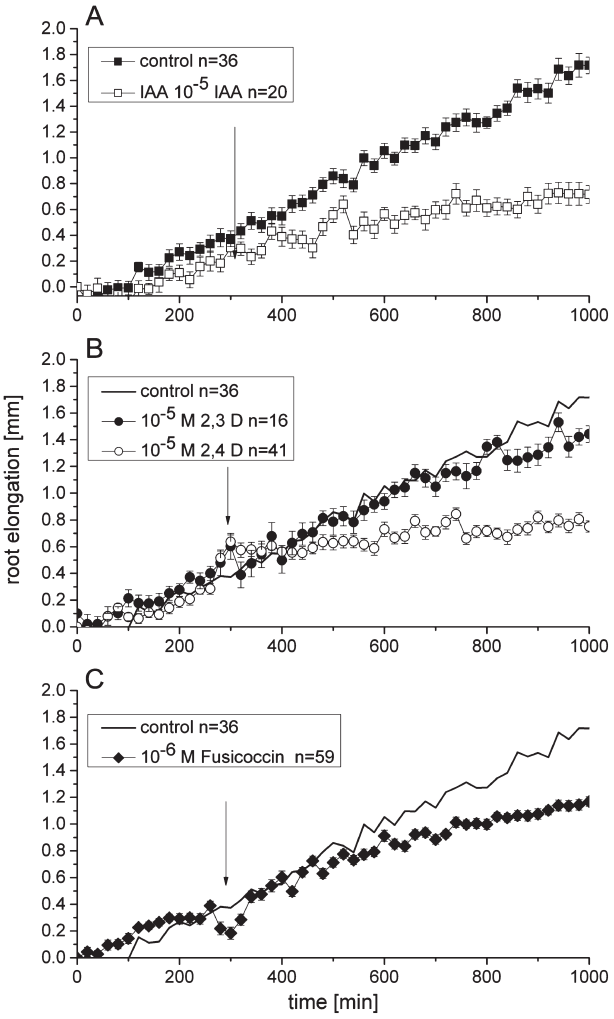

Fig. 3. Growth responses of *Arabidopsis* roots to IAA (A), 2,4-D and 2,3-D (B), and Fusicoccin (C), compared to untreated controls. Error bars indicate standard errors; the number of individual experiments is given. Note that the experiments shown (except for the controls in B and C) were made simultaneously.

reflecting probably a long-term toxic effect of the acidic pH on the segments. In maize coleoptiles, the initial rise in growth rate has been earlier shown to be short-lived. Shrinkage, however, is only observed at unphysiological pH of <3 in maize (Lüthen et al. 1990). Fig. 4D depicts FC-induced elongation in *Arabidopsis* hypocotyls. As in maize coleoptiles, the effect of FC on elongation growth was dramatic, but short-lived.

Discussion

In this paper, we present an efficient auxanometer for studying auxin responses in roots and in excised hypocotyl segments of *Arabidopsis* at high throughput. We could demonstrate that the results reflect known patterns of growth responses to auxins, fusicoccin and acidic pH (Figs 3 and 4). Use of a scanner as an imaging system was clearly a compromise, but crucial for high throughput operation. In Figs 3 and 4, the temporal resolution is limited to 20 or 10 min, respectively. For an analysis of the 10–20-min lag phases reported in transducer and CCD studies, micrographs should be used with HT, at the price of a lower throughput. This system can now be employed for studying a number of mutants at various auxin concentrations.

Systems to measure growth effects and other rapid responses in *Arabidopsis* have been developed and successfully employed by a number of labs. Hypocotyl segments were recorded by digitized video- or CCD imaging and the length of the segments were measured. In several cases, determining the changes in length was done by measuring the digital images manually (Christian and Lüthen 2000, Schenck et al. 2010); but from the beginning there have been attempts to measure the images automatically (Ishikawa et al. 1991, Evans et al. 1994). The simplest form is to detect the tip of a root or marker beads attached to the surface of the root or segment, also allowing to record gravitropic or phototropic curvature.

For higher throughput, an automatic detection of the midline of the elongating organ in an image is essential. In 2009, Wang et al. presented their software HYPOTRACE, which for the first time allowed manual and semi-automatic or even automatic operation in camera-based recordings of gravitropism in intact hypocotyls.

However, this approach called for higher degree of automation at the software side of the problem, which we achieved in this paper. The key problem turned out to be an improved detection of the midline in an image. Thresholding and thinning needed to require less user attention. Lee et al. (1994) published a useful algorithm to extract the medial axis of 2D and 3D objects. The skeletonizing algorithm has been implemented in Fiji and ImageJ plugins by Arganda-Carreras et al. (2010). After the extract of the medial axis, the longest shortest path is identified using the Floyd–Warshall algorithm (Floyd 1962, Warshall 1962). These plugins and the algorithms on which they are based have already been employed in a number of other biological and medical applications within the last 2 or 3 years like root system anatomy (Armengaud et al. 2009), bone anatomy (Doube et al. 2010) and very recently in *C. elegans* research (Moore et al. 2013).

We feel that the enhanced throughput of our system paves the way for efficiently screening and characterizing auxin response mutants in *Arabidopsis*.

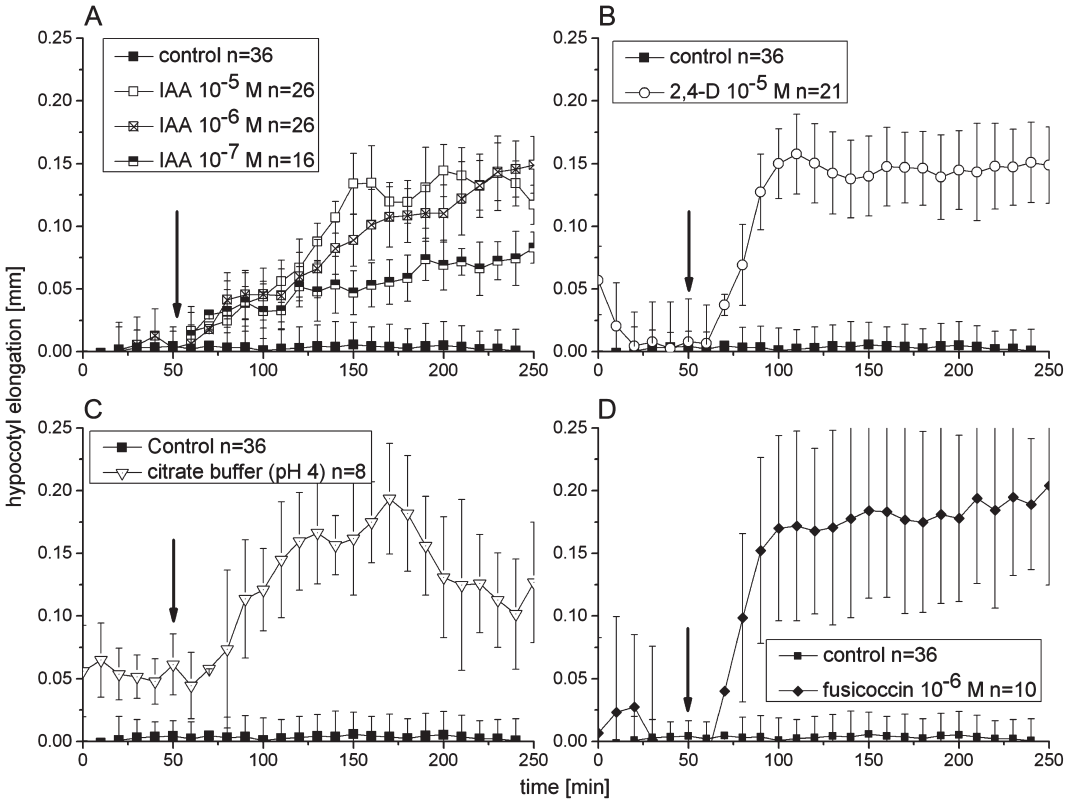

Fig. 4. Growth responses of excised hypocotyl segments to various concentrations of the endogenic auxin IAA (A), to the active auxin 2,4-D (B), to acidification to pH 4 (abraded hypocotyl segments; C) and to the fungal toxin fusicoccin (D). Error bars indicate standard errors; the number of individual experiments is given. Note that the experiments shown (except for the controls in B and C) were made simultaneously. The apparently stronger response in (B) may reflect slight differences in segment preparation.

Author contributions

This paper is based in part of MSc theses by V. N. and S. F., and a PhD thesis of S. F. in Hartwig Lüthen's group at the University of Hamburg, Germany.

Acknowledgements – S. F. was supported by a PhD student's grant by the Appuhn-Stiftung, Hamburg.

References

Arganda-Carreras I, Fernandez-Gonzalez R, Munoz-Barrutia A, Ortiz-De-Solorzano C (2010) 3D reconstruction of histological sections: application to mammary gland tissue. Microsc Res Tech 73: 1019–1029

Armengaud P, Zambaux K, Hills A, Sulpice R, Pattison RJ, Blatt MR, Amtmann A (2009) EZ-Rhizo: integrated software for the fast and accurate measurement of root system architecture. Plant J 57: 945–956

Christian M, Lüthen H (2000) New methods to analyse auxin-induced growth I: classical auxinology goes *Arabidopsis*. Plant Growth Regul 32: 107–114

Claussen M, Lüthen H, Blatt M, Böttger M (1997) Auxin induced growth and its linkage to potassium channels. Planta 201: 227–231

Cobb JN, DeClerk G, Greenberg A, Clark R, McCouch S (2013) Next-generation phenotyping: requirements and strategies for enhancing our understanding of genotype–phenotype relationships and its relevance to crop improvement. Theor Appl Genet 126: 867–887

Doube M, Klosowski MM, Arganda-Carreras I, Cordelieres FP, Dougherty RP, Jackson JS, Schmid B, Hutchinson JR, Shefelbine SJ (2010) BoneJ: Free and extensible bone image analysis in ImageJ. Bone 47: 1076–1079

Evans ML (1974) Rapid responses to plant hormones. Annu Rev Plant Physiol 25: 195–223

Evans ML, Ishikawa H, Estelle MA (1994) Responses of *Arabidopsis* roots to auxin studied with high temporal resolution: comparison of wild type and auxin response mutants. Planta 194: 215–222

Floyd RW (1962) Algorithm 97: shortest path. Commun ACM 5: 345

Ishikawa H, Hasenstein KH, Evans ML (1991) Computer-based video digitiser analysis of surface extension in maize roots. Planta 183: 381–390

Kapur JN, Sahoo PK, Wong ACK (1985) A new method for gray-level picture thresholding using the entropy of the histogram. CVGIP 29: 273–285
Lee T-C, Kashyap RL, Chu C-N (1994) Building skeleton models via 3-D surface/axis algorithms. CVGIP 56: 462–478
Lüthen H, Böttger M (1988) Kinetics of proton secretion and growth in maize roots: Action of various plant growth effectors. Plant Sci 54: 37–43
Lüthen H, Böttger M (1993) The role of protons in the auxin induced root growth inhibition: a critical reexamination. Bot Acta 106: 58–63
Lüthen H, Bigdon M, Böttger M (1990) Reexamination of the acid growth theory of auxin action. Plant Physiol 93: 931–939
Moore BT, Jordan JM, Baugh LR (2013) WormSizer: high-throughput analysis of nematode size and shape. PLoS One 8: e57142. DOI: 10.1371/journal.pone.0057142
Polder G, Hovens HLE, Zweers AL (2010) Measuring shoot length of submerged aquatic plants using graph analysis. Proceedings of the ImageJ User and Developer Conference, 27–29 Oct 2010, Centre de Recherche Public Henri Tudor, Luxembourg, pp 172–177.
Scheitz K, Lüthen H, Schenck D (2013) Rapid auxin-induced root growth inhibition requires the TIR and AFB auxin receptors. Planta 238: 1171–1176
Schenck D, Christian M, Jones A, Lüthen H (2010) Rapid auxin-induced cell expansion and gene expression: a four-decade-old question revisited. Plant Physiol 152: 1183–1185
Wang L, Uilecan IV, Assadi AH, Kozmik CA, Spalding E (2009) HYPOTrace: image analysis software for measuring hypocotyl growth and shape demonstrated on *Arabidopsis* seedlings undergoing photomorphogenesis. Plant Physiol 149: 1632–1637
Warshall S (1962) A theorem on Boolean matrices. J ACM 9: 11–12
Went FW (1928) Wuchsstoff und Wachstum. Recueil Trav Bot Neerl 25: 1–116
Zack GW, Rogers WE, Latt SA (1977) Automatic measurement of sister chromatid exchange frequency. J Histochem Cytochem 25: 741–753

Supporting Information

Additional Supporting Information may be found in the online version of this article:

Fig. S1. Workflow for the numerical treatment of control data.

Edited by K. Ljung